NONLINEAR RESPONSE OF RC BUILDINGS DUE TO IMPACT OF TSUNAMI WATER-BORNE BOATS AND CONTAINERS

Kavinda Manoj Madurapperuma[1] and Anil C. Wijeyewickrema[2]

[1] *Graduate Student, Dept. of Civil Engineering, Tokyo Institute of Technology, Tokyo, Japan*
[2] *Associate Professor, Dept. of Civil Engineering, Tokyo Institute of Technology, Tokyo, Japan*
Email: ma.k.aa@m.titech.ac.jp, wijeyewickrema.a.aa@m.titech.ac.jp

ABSTRACT:

Tsunami resistant buildings where the lower level is elevated by means of RC columns to allow the free flow of tsunami waves, have been recently constructed in some countries. However these columns are very vulnerable to impact due to water-borne massive objects. Tsunami field survey observations show that building destruction is often exacerbated by the impact of tsunami water-borne massive objects such as automobiles, barges, boats, empty storage tanks and shipping containers. In this paper, impact of tsunami water-borne massive objects on a RC building that could be used for tsunami evacuation purposes is considered using a fiber-based discretization model in OpenSEES. The building is analyzed and designed using SAP2000 prior to impact simulation. Two frame systems are considered, namely ordinary moment frame (OMF) and special moment frame (SMF) for low seismic risk zones and high seismic risk zones, respectively. Nonlinear dynamic analysis is conducted to investigate building response due to impact of boats and shipping containers. At the column impact section the displacement, shear force and moment-curvature responses are investigated. In addition, the stress-strain behavior of cover concrete, core concrete and tension reinforcement at the impact section are studied. Numerical results show that in contrast to the OMF system, the SMF system can resist the impact load without strength degradation for the range of water-borne objects that are considered.

KEYWORDS: impact loads, nonlinear dynamic analysis, reinforced concrete frames, tsunamis, water-borne objects

1. INTRODUCTION

The Indian Ocean tsunami on December 26, 2004 has resulted in massive destruction to coastal communities with more than 275,000 fatalities, and severe damage to buildings, bridges and other infrastructure causing serious socio-economic problems (DFID 2005 and Inoue et al. 2007). Many RC buildings collapsed or were severely damaged due to the impact of massive objects carried by the tsunami waves. However, tsunami field surveys have reported that even improperly designed buildings that had only columns in the first-story (i.e., no infill walls) performed well during the Indian Ocean tsunami (Dias et al. 2006). Based on tsunami field observations and research studies, new tsunami resistant buildings have been constructed, where the lower level of the building would be elevated by means of RC columns to allow the free flow of tsunami waves. An example of a recently constructed RC frame building is shown in Figure 1. However, these columns are very vulnerable to impact from tsunami water-borne massive objects such as automobiles, barges, boats, empty storage tanks and shipping containers (Ghobarah et al. 2006). Therefore, it is of paramount importance to consider the effect of such impact forces when designing buildings in tsunami inundation zones.

Building damage due to tsunami water-borne massive objects has been studied in Madurapperuma (2007) and in this paper, impact on a RC building with elevated lower level due to boats and shipping containers is discussed. Nonlinear dynamic analysis of two RC frame systems are considered, namely ordinary moment frame (OMF) and special moment frame (SMF) for low seismic risk zones and high seismic risk zones, respectively (IBC 2003). At the column impact section the displacement, shear force and moment-curvature responses are investigated. In addition, the stress-strain behavior of cover concrete, core concrete and tension reinforcement at the impact section are studied. Finally, the behavior of the OMF and SMF systems are compared.

Figure 1 A tsunami resistant building with elevated lower level in Sri Lanka

2. BUILDING DESCRIPTION AND STRUCTURAL DESIGN

The building considered is a three-story school building, located in a tsunami inundation zone that can also be used for tsunami evacuation purposes. The plan and elevation of the RC building are shown in Figure 2. The first-story is open space with only columns allowing free flow of tsunami waves. The building was analyzed and designed according to the strength design method specified in ACI 318-02 (ACI 2002) using SAP2000 (2004). Design live loads and earthquake loads were determined using code provisions of the International Building Code 2003 (IBC 2003). The design details are given elsewhere (Madurapperuma 2007).

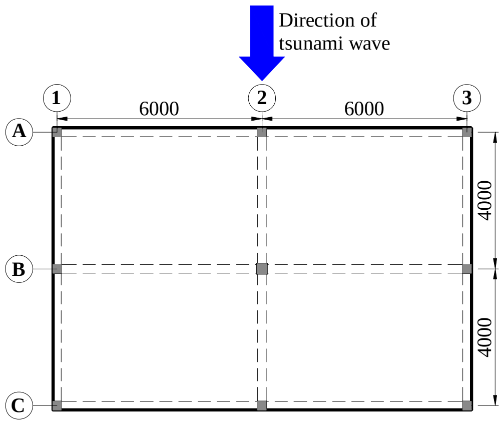

(a) Plan

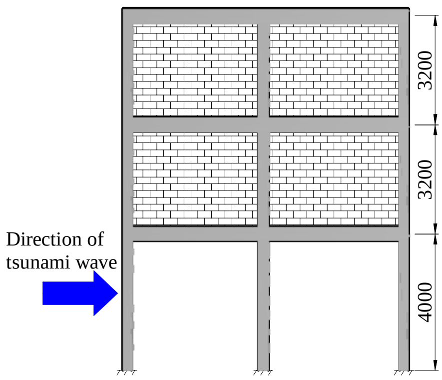

(b) Elevation

Figure 2 Building configuration used in the study (all dimensions in mm)

3. EVALUATION OF TSUNAMI FORCES

Some of the main forces acting on structures due to a tsunami are breaking wave force, buoyant force, hydrostatic force, surge force, hydrodynamic (drag) force and impact force due to water-borne objects (Yeh 2006). In the present study, the dominant forces are the hydrodynamic force and the impact force from tsunami water-borne massive objects.

3.1. Hydrodynamic Force

The hydrodynamic force F_H exerted on first-story columns can be evaluated from

$$F_H = \frac{1}{2}\rho C_D A u^2, \tag{3.1}$$

where $\rho =$ fluid mass density, $C_D =$ drag coefficient (2.0 for square columns), $u =$ tsunami flow velocity, and $A =$ wetted area of the object projected on the plane normal to the flow direction i.e., $A = hb$, in which $h =$ flow depth and $b =$ breadth of the object (FEMA 2000). The tsunami flow velocity u is calculated from the two equations,

$$\eta = \frac{1}{36\tau^2}(2\sqrt{2}\tau - \tau^2 - 2\zeta)^2, \tag{3.2}$$

$$\upsilon = \frac{1}{3\tau}(\tau - \sqrt{2}\tau^2 + \sqrt{2}\zeta), \tag{3.3}$$

where $\eta = h/R$, $\upsilon = u/\sqrt{2gR}$, $\tau = t\tan\theta\sqrt{g/R}$, $\zeta = z/R$; in which $R =$ runup, $g =$ gravitational acceleration, $t =$ time ($t = 0$ at the shoreline), $\theta =$ beach slope and $z =$ ground elevation at the location of interest measured from the shoreline (Yeh 2007). The Eqns. (3.2) and (3.3) can be used to determine υ for a given η and ζ. Out of the four possible roots for υ only the root bounded by the $\eta = 0$ curve should be taken (see Figure 3 of Yeh (2007)). It is noted that flow velocities decrease with increase in flow depth.

3.2. Impact Force

The estimation of time varying impact force on the structure is complex because the force generated during the impact is influenced by the properties of the water-borne object, e.g., material properties, geometry, mass, velocity and orientation on impact; and the properties of the structure itself, particularly its stiffness and inertia (Stronge 2000). In this study, the impact force-time history is based on the impulse-momentum approach that equates the change in linear momentum of the water-borne object and the impulse imparted on the structure during the impact. This results in the following expression for the time varying impact force F_I:

$$\int_0^{t_I} F_I \, dt = \Delta(mu^{obj}) = mu, \tag{3.4}$$

where $m =$ mass of the object, $u^{obj} =$ velocity of the object and $t_I =$ impact duration. In Eqn. (3.4) it is assumed that the velocity of the object before impact is the same as the tsunami flow velocity u for the given inundation depth and that the linear momentum of the object after impact is zero. The impact force-time history for the dynamic analysis is assumed to be of triangular shape and the impact duration is taken as $t_I = 0.1$ s following the recommendation for RC construction in CCH (2000).

4. FINITE ELEMENT MODELING OF IMPACT

Impact simulation of the two-dimensional structural frame along grid line 2 in Figure 2(a) is carried out using a fiber-based discretization model in OpenSEES (2006). The frame is modeled using the *nonlinearBeamColumn* element which is a distributed plasticity type force-based element with fiber sections accounting for the spread of plasticity both over the cross-section and along the member length. In order to accurately model the actual behavior of the column in the area that impact takes place, the deformable height of the impacted column is divided into a number of elements. Material properties for concrete and reinforcing bars are defined through conventional stress-strain models available in OpenSEES. The concrete material response is simulated using the *Concrete02* material model. The model proposed by Mander et al. (1988) is used to estimate the core concrete strength accounting for the amount of confinement provided by transverse reinforcements. The *Steel02* material model is used to simulate the steel material response. The material properties for nonlinear material modeling of concrete and reinforcing bars are given in Madurapperuma (2007).

The hydrodynamic force on a column is evaluated using Eqns. (3.1)-(3.3), and applied on the first-story columns as a uniform load from the column base to the tsunami flood level. Equations (3.2)-(3.4) are used to calculate the maximum impact force based on which the impact force-time history is obtained. The impact force is applied as a point load which is conservative with regard to response evaluation of the building.

5. NUMERICAL ANALYSIS

Nonlinear dynamic analysis is carried out with the modified Newton-Raphson iterative scheme and the Newmark method for time integration with $\beta = 0.25$, $\gamma = 0.5$. The Rayleigh damping parameters are calculated assuming a 5% damping ratio. The time step is taken as $\Delta t = 0.0005$ s for all analyses. It is assumed that the building is located 2.0 m above the shoreline and the land is inundated by a tsunami runup of 12.0 m (i.e., $z = 2.0$ m and $R = 12.0$ m). The nonlinear response of the impacted column is investigated using different masses of boats (Maxum 2007) and shipping containers (Evergreen 2007) impacting column A2 (Figure 2(a)) at 2.0 m and 2.5 m above the ground level, respectively. The draft of containers (assumed water tight) is calculated by equating the weight of the container with the buoyancy force, and the draft of boats can be found in Maxum (2007). The draft values are assumed to be the same as the flow depth h (since draft of the object must be less than or equal to the flow depth for the object to float) for estimating the tsunami flow velocity u from Eqns. (3.2) and (3.3). The tsunami flow velocities and the maximum impact forces are given in Table 1. The response of the column A2 at the impacted cross-section is studied.

Table 1 Maximum impact forces for different types of water-borne objects

Water-borne object	Dimensions (m)	Mass (kg)	Draft (m)	Velocity (m/s)	Maximum impact force (kN)
Boats	5.5×2.3^{a} $(1800\ \mathrm{SR})^{c}$	1200	0.51	8.18	196
	5.8×2.4^{a} $(1900\ \mathrm{SR})^{c}$	1500	0.56	7.81	234
Containers	$3.0 \times 2.4 \times 2.6^{b}$ $(10')^{c}$	1300	0.17	10.84	282
	$3.0 \times 2.4 \times 2.6^{b}$ $(10')^{c}$	1375	0.18	10.82	298

[a] length × beam, [b] length × width × height, [c] model type.

The impact response of the OMF system due to boats which have masses of 1200 kg and 1500 kg is considered first. The displacement, shear force and moment-curvature responses are shown in Figure 3. In Figure 3(a) the column displacement at 2.0 m above ground level attains a peak value of approximately 17 mm after 0.075 s and then decreases to a constant value of 5 mm due to impact of the 1500 kg boat. This peak displacement is more than 2.5 times the peak displacement due to impact of the 1200 kg boat at the same level. It is expected that the spalling of cover concrete followed by the yielding and buckling of steel reinforcements cause this constant displacement which is not equal to that before impact (i.e., displacement due to hydrodynamic force and gravity loads). The shear force in Figure 3(b) increases with increase in impact force up to certain magnitude and then a sudden drop of shear force can be seen for impact of the 1500 kg boat. Shear failure is expected at the impacted section during the impact loading causing strength degradation due to impact of the 1500 kg boat. To investigate flexural behavior, moment-curvature response of the impacted section is considered (Figure 3(c)). When the 1500 kg boat impacts the column, moment drops after spalling of the cover concrete and decreases with further increase in curvature forming a plastic hinge at the impacted section with extensive inelastic behavior. The reinforcements at the impacted section could have buckled or ruptured with further increase in curvature.

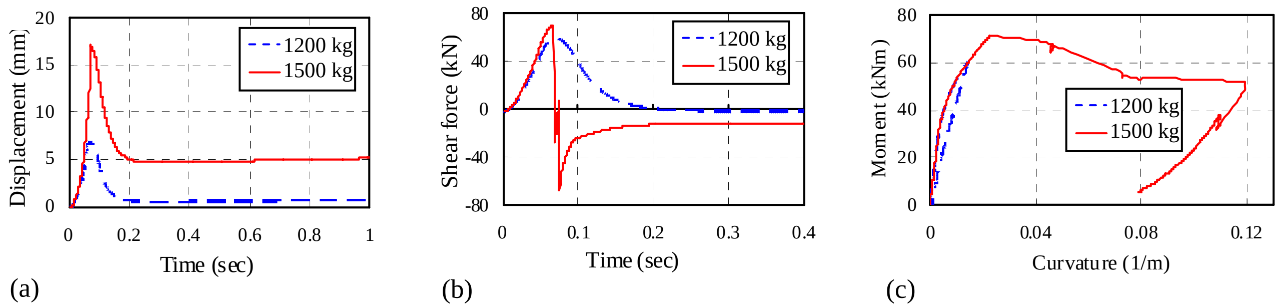

Figure 3 Response at impacted section of column A2 of OMF at 2.0 m above ground level: (a) displacement, (b) shear force and (c) moment-curvature

The stress-strain behavior of the cover concrete at extreme fibers in compression, the core concrete at extreme fibers in compression and the longitudinal bar in tension are plotted in Figure 4. When the column displacement reaches its peak value due to impact of the 1500 kg boat (Figure 3(a)), the cover concrete stress at the extreme fibers in compression exceeds the compressive strength -27.579 MPa and reaches to crushing strength -5.516 MPa at a strain of -0.0068. Since the cover concrete is not confined, the stress in cover concrete compression fibers finally becomes zero with a strain of -0.0072 (Figure 4(a)). The stress in core concrete compression fibers reaches -33.636 MPa at a strain of -0.0027 and finally becomes -20.13 MPa at a strain of -0.0022 (Figure 4(b)). The final stress of -20.13 MPa which is 4.4 times the initial stress of -4.59 MPa before impact, shows degradation of the axial load carrying capacity due to impact of the 1500 kg boat. From Figure 4(c) it can be seen that the longitudinal bar in tension has yielded and the maximum strain is 0.011 which is 5.5 times the yield strain, due to impact of the 1500 kg boat.

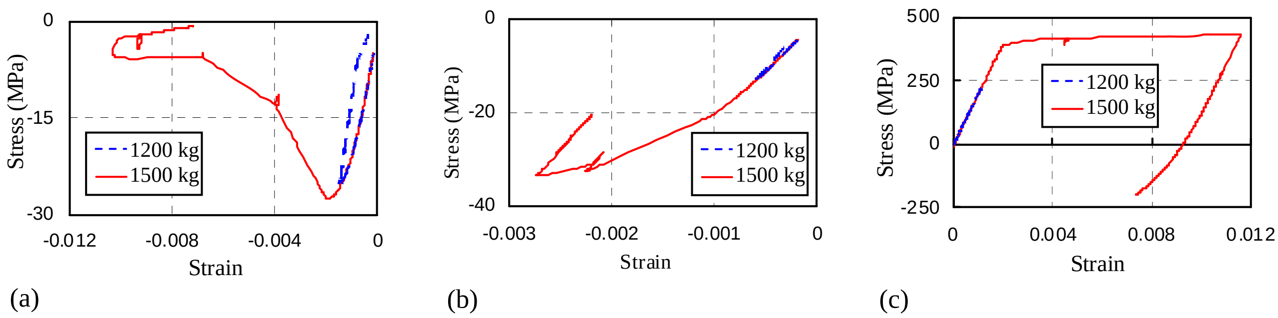

Figure 4 Stress-strain behavior of column A2 of OMF at section 2.0 m above ground level: (a) cover concrete at extreme fiber in compression, (b) core concrete at extreme fiber in compression and (c) longitudinal bar in tension

The impact response of the OMF system due to shipping containers which have masses of 1300 kg and 1375 kg impacting at 2.5 m above the ground level is considered next. It is noted that, the velocities of containers are greater than that of boats since the drafts of containers are small compared to that of boats. Therefore, the maximum impact forces due to impact of containers are greater than that of boats (see Table 1). The displacement, shear force and moment-curvature responses are shown in Figure 5. In Figure 5(a), the column displacement at 2.5 m above ground level attains a peak value of approximately 13 mm after 0.0695 s and then decreases to a constant value of 1 mm due to impact of the 1375 kg container. The peak displacement is reduced by 30% although the impact force is greater than that at 2.0 m above ground level. A sudden drop of shear force can be seen in Figure 5(b) causing strength degradation due to impact of 1375 kg container. The shear force finally equals to that before impact (i.e., shear force due to hydrodynamic force and gravity loads) showing less damage when compared to the impact at 2.0 m above ground level. In Figure 5(c), when the 1375 kg container impacts the column, the moment drops and decrease with further increase in curvature, however, the inelastic deformation is small when compared to that at 2.0 m above the ground level.

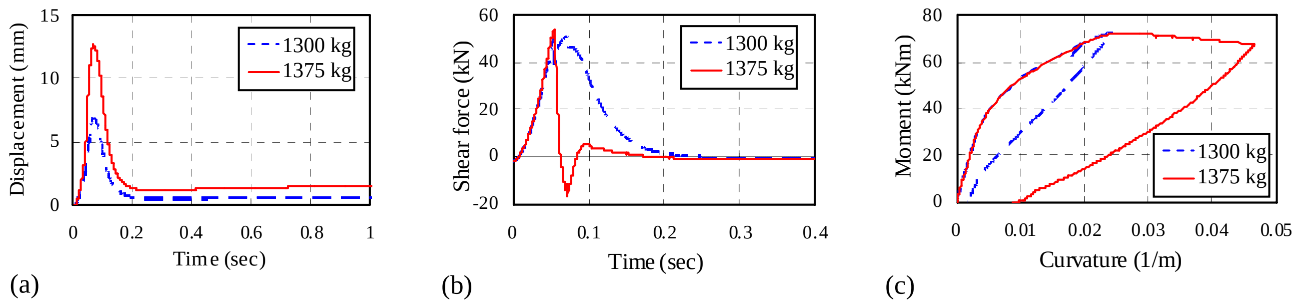

Figure 5 Response at impacted section of column A2 of OMF at 2.5 m above ground level: (a) displacement, (b) shear force and (c) moment-curvature

The stress-strain behavior of the cover concrete at extreme fibers in compression, the core concrete at extreme fibers in compression and the longitudinal bar in tension are plotted in Figure 6. In Figure 6(a), when the 1375 kg container impacts the column, the cover concrete stress at the extreme fiber in compression exceeds the compressive strength -27.579 MPa and reaches to -13.312 MPa at a strain of -0.0039. Since the cover concrete does not reach to the crushing strength, only cracking of concrete at the impacted section is expected. In Figure 6(b), the stress in core concrete compression fibers is below the compressive strength and therefore, concrete cracking is confined only to the cover concrete. Due to cracking of concrete in the tension side, the longitudinal bar in tension has yielded and the maximum strain is 0.0045 which is, however, an approximately 60% reduction compared to that at 2.0 m above the ground level (Figure 6(c)). The computed stress-strain behavior of the cover concrete, core concrete and longitudinal bar shows failure of the impacted sections in column A2 of the OMF system when impacted by the 1500 kg boat and 1375 kg container at 2.0 m and 2.5 m above the ground level, respectively. However, the impacted section at 2.5 m above the ground level shows higher impact resistance when compared to the impacted section at 2.0 m above the ground level.

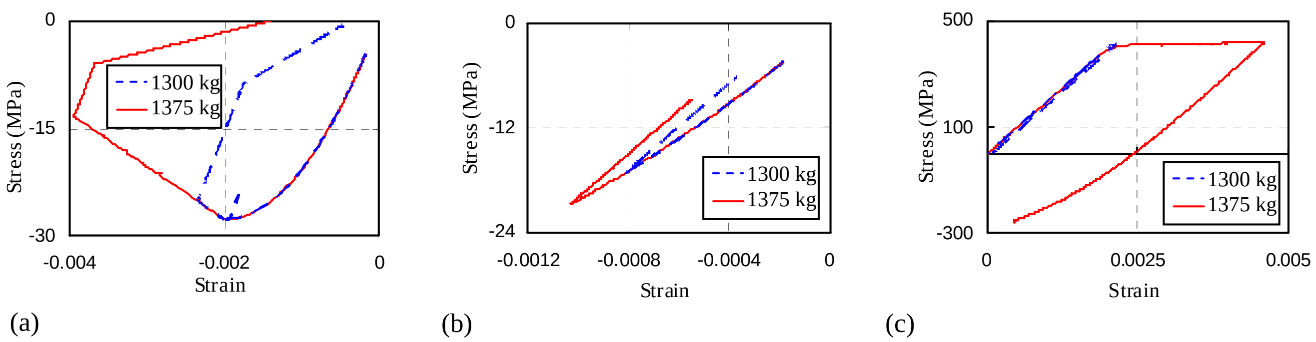

Figure 6 Stress-strain behavior of column A2 of OMF at section 2.5 m above ground level: (a) cover concrete at extreme fiber in compression, (b) core concrete at extreme fiber in compression and (c) longitudinal bar in tension

The effectiveness of the SMF system compared to the OMF system for impact resistance is considered next. The comparison is carried out by investigating the response of the column A2 at 2.0 m above the ground level (which is the most critical section for impact) when impacted by the 1500 kg boat. Figure 7 shows the displacement, shear force and moment-curvature responses for the two different systems. Use of the SMF system reduced the maximum displacement at the impacted section by approximately 80% when compared to the use of the OMF system (Figure 7(a)). The computed displacement response for the SMF system indicates that, after impact the displacement is nearly equal to that before impact (i.e., the displacement due to hydrodynamic force and gravity loads). Since the shear capacity of the SMF system is higher than that of the OMF system a sudden drop in shear force cannot be seen in Figure 7(b) for the SMF system. In Figure 7(c) it can be seen that the moment capacity at the impact section of the SMF system is increased by approximately 15% without forming a plastic hinge when compared to the OMF system.

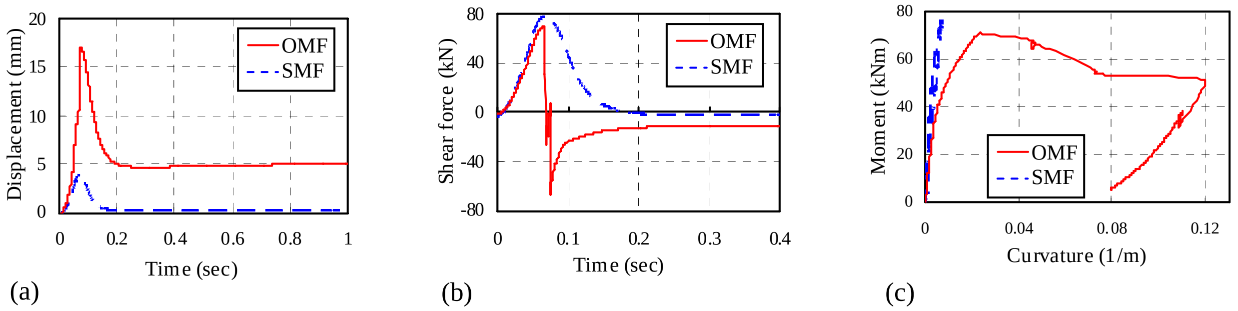

Figure 7 Response of column A2 at impacted section 2.0 m above ground level when impacted by 1500 kg boat: (a) displacement, (b) shear force and (c) moment-curvature

This behavior is also seen in Figure 8(a) and 8(b) where the stress in the cover concrete and core concrete at the extreme fiber in compression is below the compressive strength, and the strain in the tension reinforcement in Figure 8(c) is in the elastic range. Therefore, it is seen that the SMF system performs very well compared to the OMF system when impacted by boats up to 1500 kg at 2.0 m above the ground level. This also confirms that the SMF system is safe for impact of shipping containers up to 1375 kg at 2.5 m above ground level.

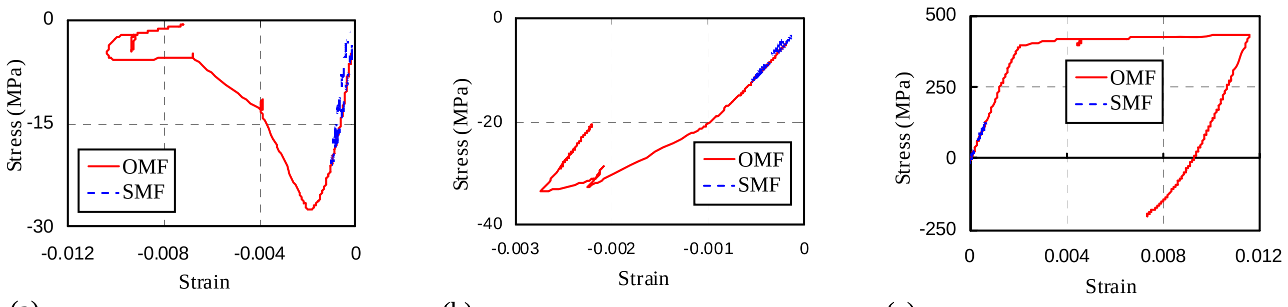

Figure 8 Stress-strain behavior of column A2 at impacted section 2.0 m above ground level when impacted by 1500 kg boat: (a) cover concrete at extreme fiber in compression, (b) core concrete at extreme fiber in compression and (c) longitudinal bar in tension

6. CONCLUDING REMARKS

The impact of tsunami water-borne massive objects on a 2D RC frame structure is considered using a fiber-based discretization model in OpenSEES. The displacement, shear force and moment-curvature responses of a first-story column is investigated where the water-borne massive objects carried by the tsunami are assumed to be boats and shipping containers. In addition, stress-strain response at impacted sections is computed to investigate concrete cracking and crushing behavior as well as inelastic behavior of steel reinforcements. It is found that impact at the mid section of the column (i.e., 2.0 m above the ground level) is more critical than impact at 2.5 m above the ground level. Numerical results show that the SMF system can resist the impact load without strength degradation for the boat and container masses considered i.e., the SMF system which provides high seismic resistance will also provide sufficient resistance against impact by boats up to 1500 kg and by containers up to 1375 kg. Hence for RC buildings in tsunami inundation zones, SMF systems will provide better resistance to impact due to water-borne massive objects than OMF systems.

Therefore, it can be concluded that impact may cause devastating damage to critical structural members of the building according to the mass of water-borne objects and the structural system. Failure of a column due to a very large impact load cannot be avoided and it would be costly to design a building for such impact loads. However, there are certain mitigation measures that could be adopted to protect critical buildings that can be used for tsunami evacuation purposes. One of the impact mitigation strategies for buildings with open first-story is the inclusion of redundancies in the open first-story to avoid collapse of the building due to failure of one or two columns. Another impact mitigation strategy is the construction of impact resisting barriers which absorb and dissipate most of the impact energy to protect critical buildings.

ACKNOWLEDGEMENTS

The first author gratefully acknowledges a Monbukagakusho scholarship from the Japanese government. The authors are very grateful to Prof. Tatsuo Ohmachi, COE Program Leader of Center for Urban Earthquake Engineering (CUEE), Tokyo Institute of Technology, and Prof. Kohji Tokimatsu, COE Program Sub-leader of CUEE, for their advice and support. Financial support from CUEE is gratefully acknowledged.

REFERENCES

American Concrete Institute (ACI). (2002). Building code requirements for structural concrete, ACI 318-02, Farmington Hills, Michigan.

CCH. (2000). Regulations within flood hazard districts and developments adjacent to drainage facilities in the revised ordinances of Honolulu, City and Country of Honolulu Building Code, Department of Planning and Permitting, Honolulu, Hawaii.

DFID. (2005). Natural disaster and disaster risk reduction measures, a desk review of costs and benefits, Department for International Development, London, <http://www.dfid.gov.uk/pubs/files/disaster-risk-reduction-study.pdf>.

Dias, P., Dissanayake, R. and Chandratilake, R. (2006). Lessons learned from tsunami damage in Sri Lanka. *Proceedings of Institution of Civil Engineers (ICE)*, **159: 2**, 74-81.

Evergreen. (2007). Container specifications, Evergreen Marine Corporation, <http://www.evergreen-marine.com/tei1/jsp/TEI1_Containers.jsp>.

Federal Emergency Management Agency (FEMA). (2000). FEMA coastal construction manual, FEMA 55, Washington, D.C.

Ghobarah, A., Saatcioglu, M. and Nistor, I. (2006). The impact of the 26 December 2004 earthquake and tsunami on structures and infrastructure. *Engineering Structures*, **28**, 312-326.

Inoue, S., Wijeyewickrema, A. C., Matsumoto, H., Miura, H., Gunaratna, P., Madurapperuma, K. M. and Sekiguchi, T. (2007). Field survey of tsunami effects in Sri Lanka due to the Sumatra-Andaman earthquake of December 26, 2004. *Pure and Applied Geophysics*, **164: 2-3**, 395-411.

International Building Code (IBC). (2003). International Code Council, Inc., Country Club Hills, Illinois.

Madurapperuma, K. M. (2007). Impact Response of Buildings due to Tsunami Water-Borne Massive Objects. M.Eng. Thesis, Dept. of Civil Engineering, Tokyo Institute of Technology, Tokyo, Japan.

Mander, J. B., Priestly, M. J. N. and Park, R. (1988). Theoretical stress-strain model for confined concrete. *Journal of Structural Engineering*, ASCE, **114: 8**, 1804-1826.

Maxum. (2007). Maxum boat models, Brunswick Corporation, <http://international.maxumboats.com/showroom.asp>.

OpenSEES. (2006). Open system for earthquake engineering simulation, <http://opensees.berkeley.edu>.

SAP2000. (2004). Integrated finite element analysis and design of structures, Computers and Structures, Inc., Berkeley, California.

Stronge, W. J. (2000). Impact mechanics, Cambridge University Press, Cambridge.

Yeh, H. (2006). Maximum fluid forces in the tsunami runup zone. *Journal of Waterway, Port, Coastal, and Ocean Engineering*, ASCE, **132: 6**, 496-500.

Yeh, H. (2007). Design tsunami forces for onshore structures. *Journal of Disaster Research*, **2**: **6**, 531-536.